Molecular Therapy
Original Article

Rescue of auditory function by a single administration of AAV-*TMPRSS3* gene therapy in aged mice of human recessive deafness DFNB8

Wan Du,[1,2,3,7] Volkan Ergin,[1,2,3,7] Corena Loeb,[1,2,3] Mingqian Huang,[1,2,3] Stewart Silver,[1,2,3] Ariel Miura Armstrong,[1,2,3] Zaohua Huang,[4] Channabasavaiah B. Gurumurthy,[5] Hinrich Staecker,[6] Xuezhong Liu,[4,7] and Zheng-Yi Chen[1,2,3,7]

[1]Department of Otolaryngology-Head and Neck Surgery, Graduate Program in Speech and Hearing Bioscience and Technology, Harvard Medical School, Boston, MA 02115, USA; [2]Department of Otolaryngology-Head and Neck Surgery, Graduate Program in Neuroscience, Harvard Medical School, Boston, MA 02115, USA; [3]Eaton-Peabody Laboratories, Massachusetts Eye and Ear, Boston, MA 02114, USA; [4]Department of Otolaryngology, University of Miami Miller School of Medicine, Miami, FL 33136, USA; [5]Mouse Genome Engineering Core Facility, University of Nebraska Medical Center, Omaha, NE 68198, USA; [6]Kansas University Center for Hearing and Balance Disorders, Kansas City, KS 66160, USA

Patients with mutations in the *TMPRSS3* gene suffer from recessive deafness DFNB8/DFNB10. For these patients, cochlear implantation is the only treatment option. Poor cochlear implantation outcomes are seen in some patients. To develop biological treatment for *TMPRSS3* patients, we generated a knockin mouse model with a frequent human DFNB8 *TMPRSS3* mutation. The *Tmprss3*$^{A306T/A306T}$ homozygous mice display delayed onset progressive hearing loss similar to human DFNB8 patients. Using AAV2 as a vector to carry a human *TMPRSS3* gene, AAV2-h*TMPRSS3* injection in the adult knockin mouse inner ear results in *TMPRSS3* expression in the hair cells and the spiral ganglion neurons. A single AAV2-h*TMPRSS3* injection in *Tmprss3*$^{A306T/A306T}$ mice of an average age of 18.5 months leads to sustained rescue of the auditory function to a level similar to wild-type mice. AAV2-h*TMPRSS3* delivery rescues the hair cells and the spiral ganglions neurons. This study demonstrates successful gene therapy in an aged mouse model of human genetic deafness. It lays the foundation to develop AAV2-h*TMPRSS3* gene therapy to treat DFNB8 patients, as a standalone therapy or in combination with cochlear implantation.

INTRODUCTION

Hearing loss (HL) is one of the most common sensory deficit disorders that affect about 466 million people.[1] Expected to afflict 1 in 10 individuals by 2050, HL poses a social and emotional toll, and a growing worldwide annual economic burden.[1] HL has been linked to increased instances of social isolation and higher risk for dementia and depression.[2,3] Genetic HL affects 1 in 500 newborns. There are no treatments available to reverse or prevent genetic deafness.[4,5] Currently hearing aids and cochlear implantation (CI) are the only treatment options, and these require residual hearing function or the ability to stimulate the cochlear nerve, respectively. While genetic HL patients can benefit from CI, those patients with ganglion deficits will be left without any treatment option.

Rapid progress has been made in the understanding of the genetic etiology of human HL.[6] Genetic testing and diagnosis of HL provide essential information for further genetic therapies.[7,8] Adeno-associated virus (AAV), a non-replicative viral vector with low immunogenicity and little ototoxicity, is one of the most promising gene therapy tools for transducing broad cellular tropism.[9,10] Gene therapies including gene editing, which can replace, edit, or silence genes, offer a promising avenue for treatment. Among them, gene replacement is appropriate for treating recessive monogenic disorders and has achieved the most clinical success, e.g., Luxturna[11] for Leber's congenital amourosis (an inherited retinal disease) and Zolgensma[12] for spinal muscular atrophy. As the inner ear is an isolated organ that can be accessed safely by local injection, a number of gene replacement and overexpression studies targeting HL have been conducted successfully, resulting in hearing rescue and the survival of hair cells (HC) or spiral ganglion neurons (SGN).[13–35]

However, with the exception of *Otof*,[25] all the gene therapy studies were performed in neonatal animals, which raises the question of the suitability of the approach in the fully mature adult inner ear.

TMPRSS3 protein, a type II transmembrane serine protease, is necessary for normal hearing in mammals. *TMPRSS3* gene mutations

Received 8 December 2022; accepted 4 May 2023;
https://doi.org/10.1016/j.ymthe.2023.05.005.

[7]These authors contributed equally

Correspondence: Xuezhong Liu, Department of Otolaryngology, University of Miami Miller School of Medicine, 1120 NW 14th St. Miami, FL 33136
E-mail: x.liu1@med.miami.edu
Correspondence: Zheng-Yi Chen, Eaton-Peabody Laboratories, Massachusetts Eye & Ear, 243 Charles St, Boston 02114
E-mail: zheng-yi_chen@meei.harvard.edu

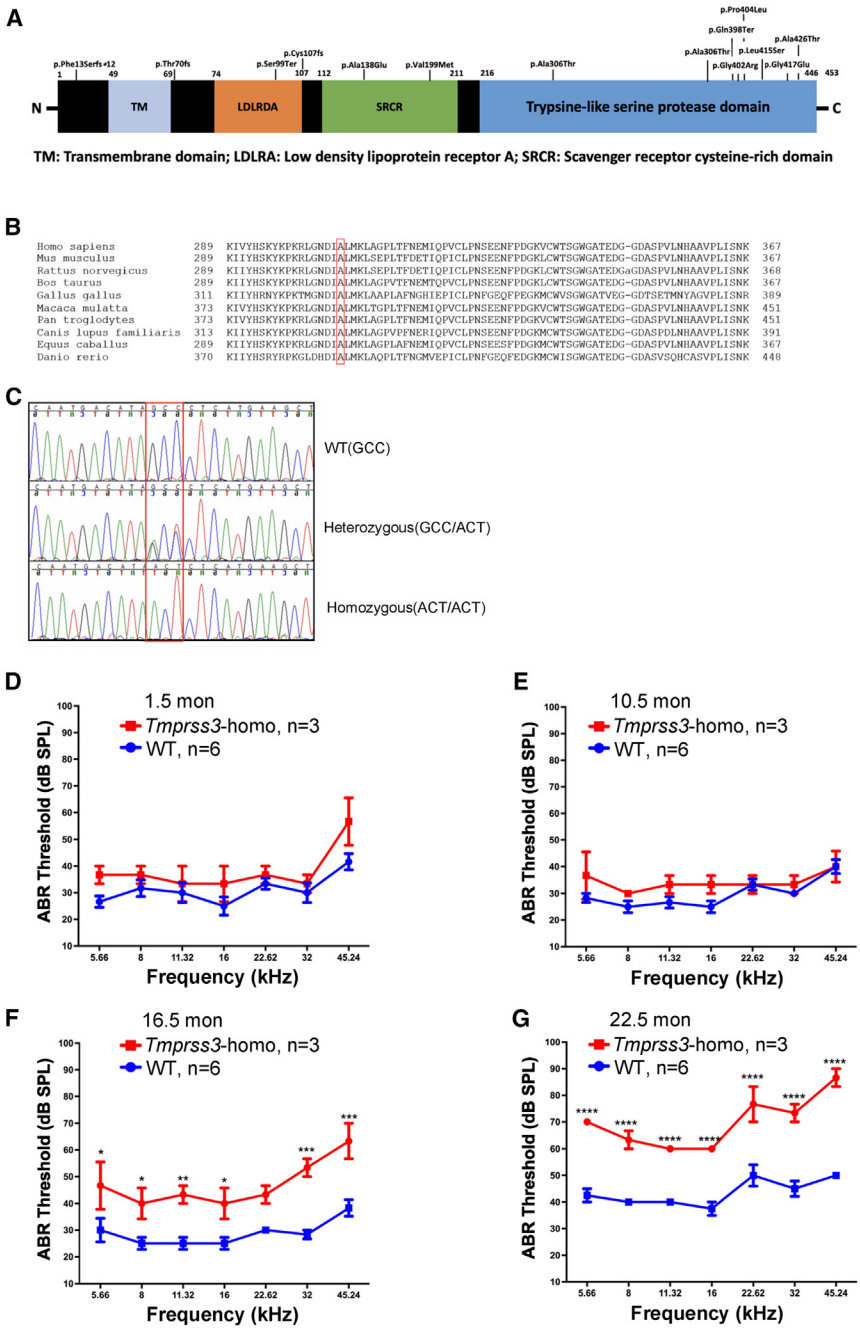

Figure 1. Generation of *Tmprss3* p.A306T KI mouse model with late-onset progressive hearing loss

(A) Summary of human TMPRSS3 protein domains and mutations. (B) Conservation of the 306 alanine from human to zebrafish species. (C) Sanger sequencing of *TMPRSS3* c.916G>A;c.918C>T mutant mice. (D–G) ABR thresholds in *Tmprss3*$^{A306T/A306T}$ homozygous mice ears (red) compared with wild-type ears (blue) at 1.5 months (D), 10.5 months (E), 16.5 months (F), and 22.5 months (G), respectively. Significant hearing loss by the elevated ABR thresholds was seen at 16.5 months, which became more severe at 22.5 months. Values and error bars reflect mean ± SEM.

account for approximately 12%–13% of HL families that are negative for common genetic mutations.[36,37] Two different phenotypes were present in individuals with *TMPRSS3* mutations: prelingual (DFNB10, OMIM 605511) and the delayed onset and postlingual (DFNB8, OMIM 601072).[38] A previous study has shown TMPRSS3 as a necessary permissive factor for cochlear hair cell activation and survival upon the onset of hearing loss.[39] Mice with truncated *Tmprss3* protease domains of mutation *Tmprss3*^{Y260X} showed congenital HL, and rapid loss of HC and progressive loss of SGN.[39]

To develop a mouse model with a *TMPRSS3* mutation suitable for gene therapy intervention, we constructed a DFNB8 mouse model with a knockin (KI) of a human *TMPRSS3* mutation (c.916G>A, Ala306→Thr), which causes adulthood onset and progressive recessive HL. We show by injection in aged mice, a human *TMPRSS3* gene carried by an AAV2 is re-expressed in the HC and the modiolus region. *TMPRSS3* inner ear delivery rescues hearing in aged KI mice, concomitant with the survival of HC and SGN.

RESULTS

Generation of *Tmprss3* p.A306T KI mouse model

The *TMPRSS3* gene has 13 exons and encodes a protein that consists of 453 amino acids (aa), containing four domains (Figure 1A). A human *TMPRSS3* mutation in Ala306 identified in HL patients is associated with DFNB8/10.[40–44] Ala306 is highly conserved across species from zebrafish to humans (Figure 1B). We chose to use the inbred strain of CBA/CaJ to create a KI mouse model as CBA/CaJ does not suffer from age-related hearing loss (ARHL), as in the strain of C57BL/6J, and will allow us to analyze the rescue effect over an extended period of time.[45] We used CRISPR-Cas9 technology[46–49] to create a KI mutation c.916G>A, which changed Ala to Thr at amino acid position 306 (p.A306T). In brief, to introduce mutations of Tmprss3 c.916G>A;918 C>T, i.e., p.Ala306Thr, a ribonucleoprotein complex of Cas9 protein and UGGCUCGGACAGCUUCAUGA guide RNA with the donor oligonucleotide of ACAGCAAGTACAAGCCAAAGCGGCTGGGCAA TGACATAACTC.

TCATGAAGCTTTCCGAGCCACTCACCTTTGACGAGACCATC CAGCC were injected into CBA/CaJ zygotes (Jackson Laboratory, stock no. 000656). The microinjected zygotes were then transferred

into pseudo-pregnant females.[49] The target genomic DNA region from the founder was amplified and sequenced using PCR primer pairs of: Tmprss3F, GGAGATCCCACATCTCTCACC; and Tmprss3R, AAATGCTATGCACCTACATCAAC. After the mutations were confirmed by sequencing, founder mice carrying the mutations were mated to generate wild-type (WT), heterozygous, and homozygous mutation mice. A representative mouse genotyping determined by Sanger sequencing is shown in Figure 1C.

Tmprss3$^{A306T/A306T}$ mice display late-onset progressive HL

With the aim of rescuing auditory function in the *Tmprss3*$^{A306T/A306T}$ mice, we first performed auditory brain stem response (ABR) (representing sound-evoked neural output of the cochlea) and distortion product otoacoustic emission (DPOAE) (measurement of outer hair cell function) tests to study hearing in *Tmprss3*$^{A306T/A306T}$ mice (Figures 1D–1G and S1). We found that there was no change in ABR/DPOAE thresholds or ABR wave1 amplitudes in the *Tmprss3*$^{A306T/A306T}$ ears compared with the WT CBA/CaJ ears across all frequencies at 1.5 and 10.5 months (Figures 1D, 1E, and S1A–S1D). By 16.5 months, the ABR thresholds were significantly elevated in the *Tmprss3*$^{A306T/A306T}$ ears by an average of 15 dB compared with WT ears across most frequencies (Figure 1F). DPOAE thresholds were significantly elevated at 45 kHz and wave 1 amplitudes showed significant reductions at 32 kHz with 80- and 90-dB sound pressure level (SPL) stimulation (Figures S1E and S1F). At 22.5 months, ABR thresholds were significantly elevated by an average of 26 dB across all frequencies (Figure 1G). We did not find changes in wave 1 amplitudes in *Tmprss3*$^{A306T/A306T}$ ears compared with WT ears at 22.5 months (Figure S1H), as both were much lower than that at 16.5 months (Figure S1F), an indication that neuronal activities were reduced in the WT mice due to aging. The DPOAE thresholds were elevated in *Tmprss3*$^{A306T/A306T}$ ears compared with WT ears at 22.5 months (Figure S1G). These results showed late-onset progressive HL that started after 10.5 months with significantly elevated ABR/DPOAE thresholds and reduction in wave 1 amplitudes at 16.5 months, which further deteriorated by age 22.5 months.

Designing an AAV-*TMPRSS3* gene therapy strategy

The phenotype of late onset and progressive HL in the *Tmprss3*$^{A306T/A306T}$ KI mice supports the development of a gene therapy strategy to rescue hearing in adult mouse cochleae that is clinically relevant. We chose to use AAV2 for delivery to evaluate gene therapy in the *Tmprss3*$^{A306T/A306T}$ mice as AAV2 transduces the inner hair cells (IHCs) and the outer hair cells (OHCs) with high efficiency: AAV2 transduced all the IHCs and a majority of OHCs in the apex and mid-turn with a slight reduction in the base turn in adult mouse cochlea (Figure S2). The size of the *TMPRSS3* gene is less than 1.5 kb, making it ideal for AAV-mediated delivery strategy. We cloned the coding sequences (CDSs) of mouse-*Tmprss3* (m*Tmprss3*) into the AAV2 backbone to produce AAV2-m*Tmprss3* (Figure 2A). To evaluate the potential functional ototoxicity of AAV2-m*Tmprss3*, we injected the AAV2-m*Tmprss3* into the 1-month-old WT mice and tested hearing by ABR and DPOAE 4 weeks later. To our surprise, we found that ABR thresholds were significantly elevated by an average of 35 dB across all frequencies in AAV2-m*Tmprss3*-injected ears compared with uninjected ears (Figure 2B). Similarly, there was a complete loss of DPOAE across frequencies in the injected ears (Figure 2C). Significant ABR threshold shifts and the loss of DPOAE indicated major damage by AAV2-m*Tmprss3* to the mouse inner ear. To study the cellular ototoxicity by AAV2-m*Tmprss3*, we quantified the number of OHCs and IHCs by whole-mount labeling of AAV2-m*Tmprss3*-injected ears and uninjected contralateral ears. There was a slight reduction in IHCs in AAV2-m*Tmprss3*-injected ears compared with uninjected ears, especially in the middle and basal turns (Figures 2D and 2F). There was a significant reduction in the number of OHCs across the entire cochlear turn, with the base turn being most severely affected in AAV2-m*Tmprss3*-injected ears (Figures 2E and 2G). These results demonstrate that AAV2-m*Tmprss3* induces ototoxicity by preferentially damaging OHCs, resulting in profound HL.

While we do not know the origin of the toxicity mediated by mouse *Tmprss3*, one approach to circumvent the issue is to test the use of the human *TMPRSS3* (h*TMPRSS3*) gene for delivery, as the human *TMPRSS3* gene will be used in the clinic. We constructed an AAV2-h*TMPRSS3* (Figure 2H) and injected it into 2-month-old WT mouse inner ears and performed hearing tests and inner ear characterization 4 weeks later. In the injected ears, the ABR threshold showed a similar profile to uninjected inner ears (Figure 2I). DPOAE thresholds in the injected ears were slightly elevated but were not significantly greater than uninjected ears (Figure 2J). There was no change in the number of IHCs and OHCs in AAV2-h*TMPRSS3*-injected compared to uninjected ears (Figures 2K–2N). Taken together, we conclude that the AAV2-h*TMPRSS3* inner ear delivery did not impair normal hearing or damage HC, and thus AAV2-h*TMPRSS3* is suitable for gene therapy in the *Tmprss3*$^{A306T/A306T}$ mouse model.

AAV2-mediated *TMPRSS3* expression in HC and SGN of mouse cochlea

The expression of *Tmprss3* gene or the localization of TMPRSS3 protein is not well studied in adult mouse inner ear. To study the expression pattern of *Tmprss3* in adult mouse inner ear and to evaluate the expression of the human *TMPRSS3* gene as the result of AAV2-mediated delivery, we performed RNA-FISH (fluorescence *in situ* hybridization) (RNAscope)[50,51] to detect mouse *Tmprss3* and human *TMPRSS3* genes, respectively. In WT mouse inner ear, a probe against the mouse *Tmprss3* mRNA showed strong hybridization to the endogenous *Tmprss3* mRNA that was primarily in the cochlear HC (MYO7A^{+}) in the sensory epithelium (Figure 3A). We then used a human *TMPRSS3* probe for RNAscope in WT mouse inner ear and did not detect significant signals above the background (Figure 3B). We quantified the hybridization signals by ImageJ. In WT mouse inner ear, the endogenous *Tmprss3* mRNA was expressed at a higher level in the IHCs than the OHCs, whereas no human *TMPRSS3* signals were detected (Figure 3E). Our data show that the human *TMPRSS3* probe does not cross-react with the mouse *Tmprss3* mRNA, demonstrating the specificity of the human *TMPRSS3* probe.

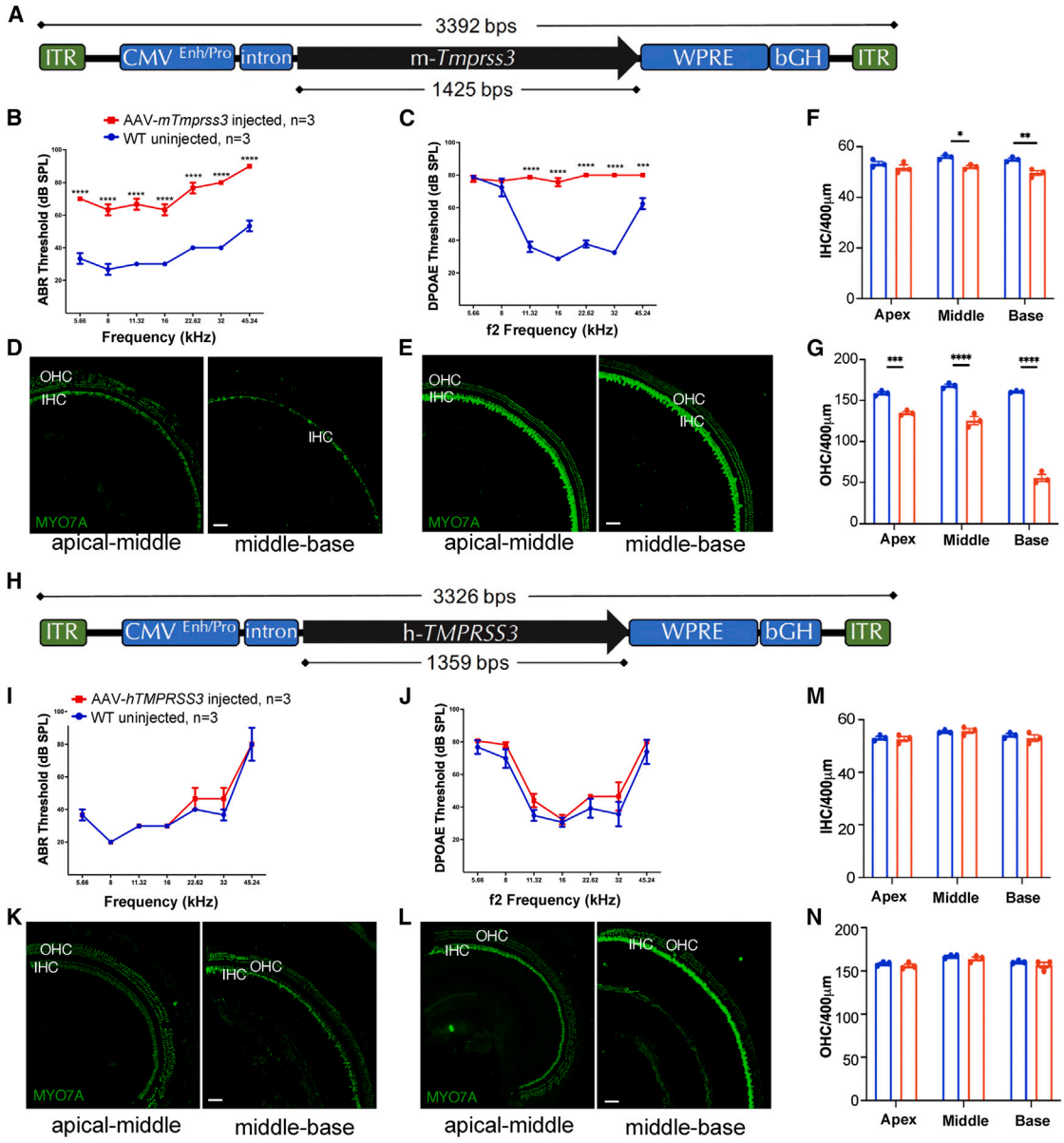

Figure 2. AAV2-h*TMPRSS3* gene therapy design strategy

(A) The construct of AAV-m*Tmprss3*. (B) ABR thresholds were significantly elevated in WT mice ears injected with AAV2-m*Tmprss3* (red) compared with uninjected ears (blue). Time of injection: age 1 month of age. Time of testing: age 2 months. (C) DPOAE thresholds were no longer detectable in WT mice ears injected with AAV2-m*Tmprss3* (red) compared with uninjected ears (blue). Time of injection: age 1 month. Time of testing: age 2 months. (D) In an injected WT cochlea, major OHC loss and some IHC loss were seen in the middle-base turn, whereas some OHC loss was seen in the apical-middle turn. MYO7A labels HC. (E) In the uninjected contralateral ear, a full set of OHCs and IHCs were seen along the cochlear turns. Scale bar, 50 μm. (F and G) Quantification of IHCs (F) and OHCs (G) per 400-μm section for three injected (red) and uninjected (blue) cochleae from three mice. Time of injection: age 1 month. Time of imaging: age 2 months. (H) The construct of AAV-h*TMPRSS3*. (I) ABR thresholds in WT mice ears injected with AAV2-h*TMPRSS3* (red) compared with uninjected ears (blue). Time of injection: age 2 months. Time of testing: age 3 months. (J) DPOAE thresholds in WT mice ears injected with AAV2-h*TMPRSS3* (red) compared with uninjected ears (blue). Time of injection: age 2 months. Time of testing: age 3 months. (K) A full set of OHCs and IHCs were seen in an AAV2-h*TMPRSS3*-injected WT ear along the cochlear turn. (L) The contralateral uninjected inner ear showed a full set of OHCs and IHCs. Scale bar, 50 μm. (M and N) Quantification of IHCs (M) and OHCs (N) per 400-μm section for three injected (red) and uninjected (blue) cochleae from three mice. Time of injection: age 2 months. Time of imaging: age 3 months. Values and error bars reflect mean ± SEM.

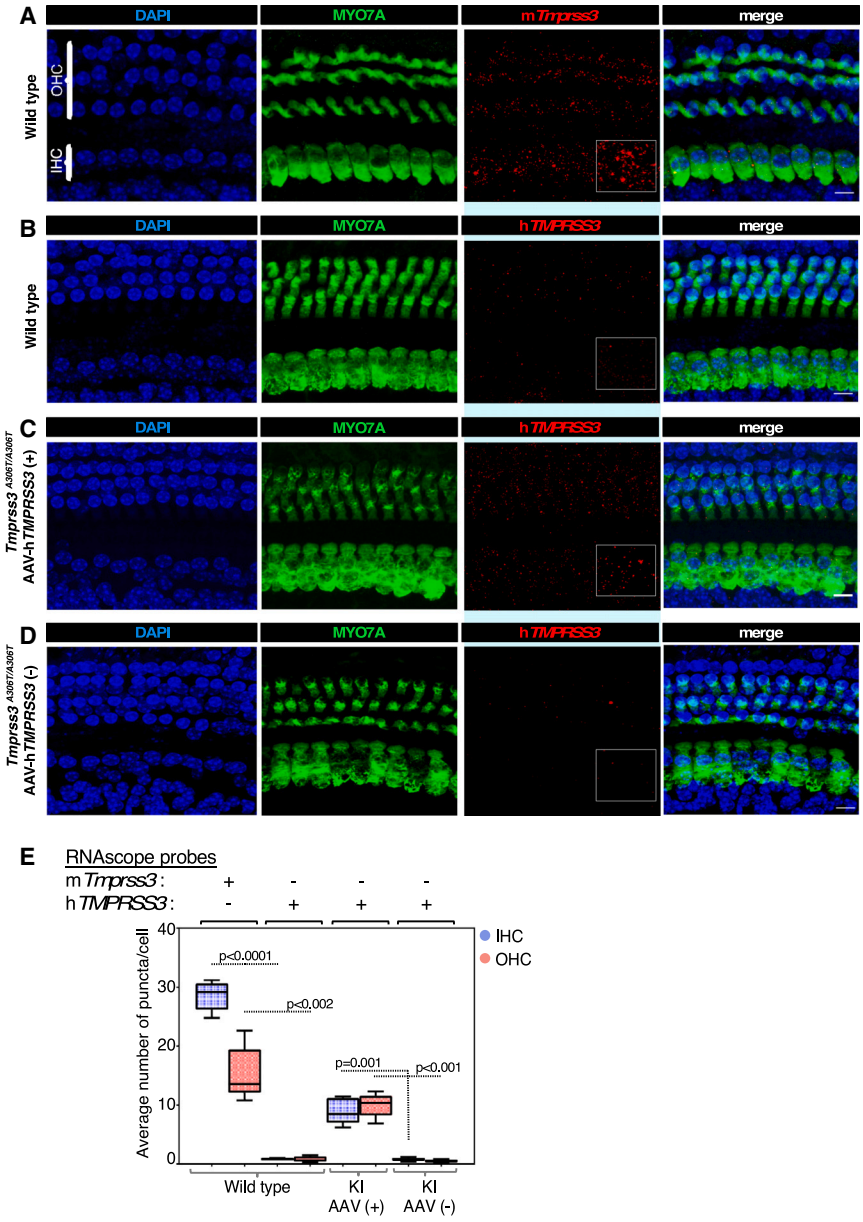

Figure 3. AAV2-h*TMPRSS3* inner ear delivery recapitulated endogenous *Tmprss3* expression in HC in *Tmprss3*$^{A306T/A306T}$ KI mice

(A) Endogenous mouse *Tmprss3* gene expression in WT mouse cochlea was detected by a mouse *Tmprss3* probe using RNAscope in a pattern overlapping with the inner and outer hair cells (IHCs and OHCs). (B) In WT mouse cochlea, a human *TMPRSS3* probe showed very low or no cross-reactivity with the endogenous mouse *Tmprss3* mRNA. (C) In a *Tmprss3*$^{A306T/A306T}$ mouse cochlea injected with AAV2-h*TMPRSS3*, a human *TMPRSS3* probe detected the transgene expression of the human *TMPRSS3* mRNA in the IHCs and OHCs. (D) In a *Tmprss3*$^{A306T/A306T}$ mouse cochlea without injection, a human *TMPRSS3* probe did not detect mRNA above the background by RNAscope. Positive signals by RNAscope are shown as red punctuates on a black background. HC were labeled with MYO7A. The white square marks the area with higher magnification for better visualization. Scale bars, 10 μm. (E) Quantification of mouse Tmprss3 or human *TMPRSS3* mRNA per IHC and OHC by RNAscope. Data are from five z stack images obtained from the apex and/or apex-mid turn regions of each sample group (control n = 3, AAV n = 2). Results are expressed as an average number of dots per IHC and OHC and are displayed as a scatter column plot with medians indicated by the horizontal bar. p values are shown on top of each dashed line between compared groups. Time of injection: age 80 weeks. Time of imaging: age 86 weeks. The RNAscope images were optimized individually for display purposes. Unpaired t-Test with Welch's correction was used to compare average number of puncta per cell between samples. Data represent mean ± SEM. Significance threshold was set as $p < 0.05$.

We then injected AAV2-h*TMPRSS3* into the *Tmprss3*$^{A306T/A306T}$ mouse inner ear and performed RNAscope. RNAscope showed that the *TMPRSS3* mRNA signals became clearly visible in the HC (Figure 3C) compared with uninjected cochlea, where no signal was detected (Figure 3D) for the same animal by the same probe. Quantification showed that a similar level of human *TMPRSS3* transgene expression was detected in the IHCs and OHCs of injected *Tmprss3*$^{A306T/A306T}$ (Figure 3E), whereas the overall *TMPRSS3* transgene expression level was lower than the endogenous *Tmprss3* mRNA in WT mouse inner ear (Figures 3A, 3C, and 3D). This study confirmed species-specific probes for *TMPRSS3*/*Tmprss3* mRNA analyses by the RNAscope method.

The failure of cochlear implant in some *TMPRSS3* patients suggests that the SGN were affected by *TMPRSS3* mutations. However, it is not known if *TMPRSS3* is expressed in the adult SGN or if any defect in the SGN is the direct result of the lack of *TMPRSS3* expression in the neurons or an indirect result of other cells that lack *TMPRSS3* expression. We examined the RNAscope data in the modiolus region that houses the SGN . RNAscope showed a distinct expression pattern of endogenous *Tmprss3* mRNA by the mouse *Tmprss3* probe in the modiolus region with the level lower than in HC (Figure 4A). Combined with the immunofluorescence staining of HuD proteins to visualize SGN soma, the *Tmprss3* expression largely overlapped with the SGN (Figure 4A). Signals were also detected in the region outside the SGN , suggesting that *Tmprss3* is expressed in other cell types in the modiolus region such as Schwann cells and satellite cells (Figure 4A). Again, the human *TMPRSS3* probe did not show signals above the background in the WT mouse modiolus region (Figure 4B), consistent with the specificity of the probe against human *TMPRSS3* mRNA.

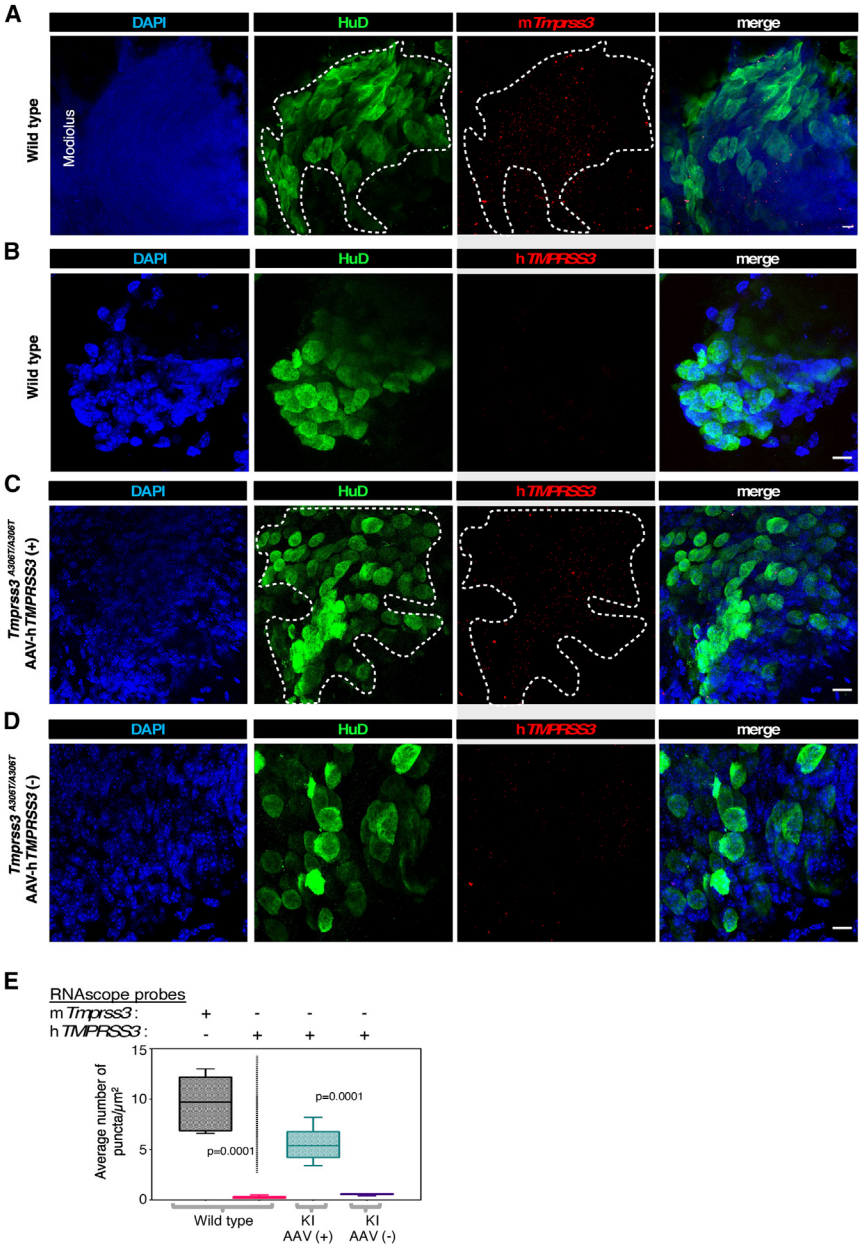

Figure 4. AAV2-h*TMPRSS3* inner ear delivery recapitulated endogenous *Tmprss3* expression in SGN in *Tmprss3*$^{A306T/A306T}$ KI mice

(A) In the WT mouse modiolus, endogenous mouse *Tmprss3* gene expression was detected by a mouse *Tmprss3* probe using RNAscope in a pattern largely overlapping with the SGN (HuD, dotted cycle). (B) In the WT mouse modiolus, a human *TMPRSS3* probe showed no cross-reactivity with the endogenous mouse *Tmprss3* mRNA. (C) In *Tmprss3*$^{A306T/A306T}$ mouse modiolus injected with AAV2-h*TMPRSS3,* a human *TMPRSS3* probe detected the transgene expression of the human *TMPRSS3* mRNA in the SGN (HuD, dotted cycle). (D) In *Tmprss3*$^{A306T/A306T}$ mouse modiolus without injection, a human *TMPRSS3* probe did not detect mRNA above the background by RNAscope. Scale bars, 10 μm. (E) Quantification of mouse *Tmprss3* or human *TMPRSS3* mRNA in the modiolus region from the above-described samples. Data are from five z stack images obtained from the apex and/or apex-mid turn regions of each sample group (control n = 3, AAV n = 2). Results are expressed as an average number of dots per modiolus and are displayed as a scatter column plot with medians indicated by the horizontal bar. p values are shown on top of each dashed line between compared groups. Time of injection: age 80 weeks. Time of imaging: age 86 weeks. The RNAscope images were optimized individually for display purposes.Unpaired t-Test with Welch's correction was used to compare average number of puncta per cell between samples. Data represent mean ± SEM. Significance threshold was set as $p < 0.05$.

We analyzed the RNAscope results of the human *TMPRSS3* probe hybridized to the *Tmprss3*$^{A306T/A306T}$ inner ear injected with AAV2-h*TMPRSS3.* We detected the expression of the human *TMPRSS3* transgene in the modiolus that overlapped with the SGN in AAV2-h*TMPRSS3*-injected *Tmprss3*$^{A306T/A306T}$ inner ear (Figure 4C), which coincided with the *Tmprss3* expression pattern in WT mice, supporting that AAV2 targeted the SGN . In uninjected contralateral *Tmprss3*$^{A306T/A306T}$ inner ear, no *TMPRSS3* expression was detected above the background (Figure 4D). Quantification confirmed that the human *TMPRSS3* gene was expressed, although at a level lower than the endogenous *Tmprss3* expression (Figure 4E). The RNAscope study showed that the endogenous *Tmprss3* is expressed in the HC and SGN in WT inner ear, and AAV2-h*TMPRSS3*-mediated gene delivery targeted the same cell population in the *Tmprss3*$^{A306T/A306T}$ inner ears with the expression of the human *TMPRSS3* gene.

AAV2-h*TMPRSS3* gene therapy rescues hearing in *Tmprss3*$^{A306T/A306T}$ mice

We performed inner ear AAV2-h*TMPRSS3* injection by round window injection with canal fenestration[52] in *Tmprss3*$^{A306T/A306T}$ mice with an average age of 18.5 months, tested hearing 1 month after injection, and continued the testing monthly for 5 months (Figure 5A). Uninjected contralateral ears served as controls. WT CBA/CaJ mice at comparable ages were tested as additional controls to show the normal hearing profile in the mouse strain during aging. Representative ABR wave forms recorded from a *Tmprss3*$^{A306T/A306T}$ homozygous mutant mouse ear, an AAV2-h*TMPRSS3*-treated *Tmprss3*$^{A306T/A306T}$ ear, and a WT mouse ear were shown at age 20.5 months, using 11.32 kHz tone bursts at incrementally increasing SPLs from 20 to 90 dB (Figure S3A). One month after injection, overall lower ABR thresholds were detected in injected ears compared with uninjected control ears at frequencies of 5.66, 16,

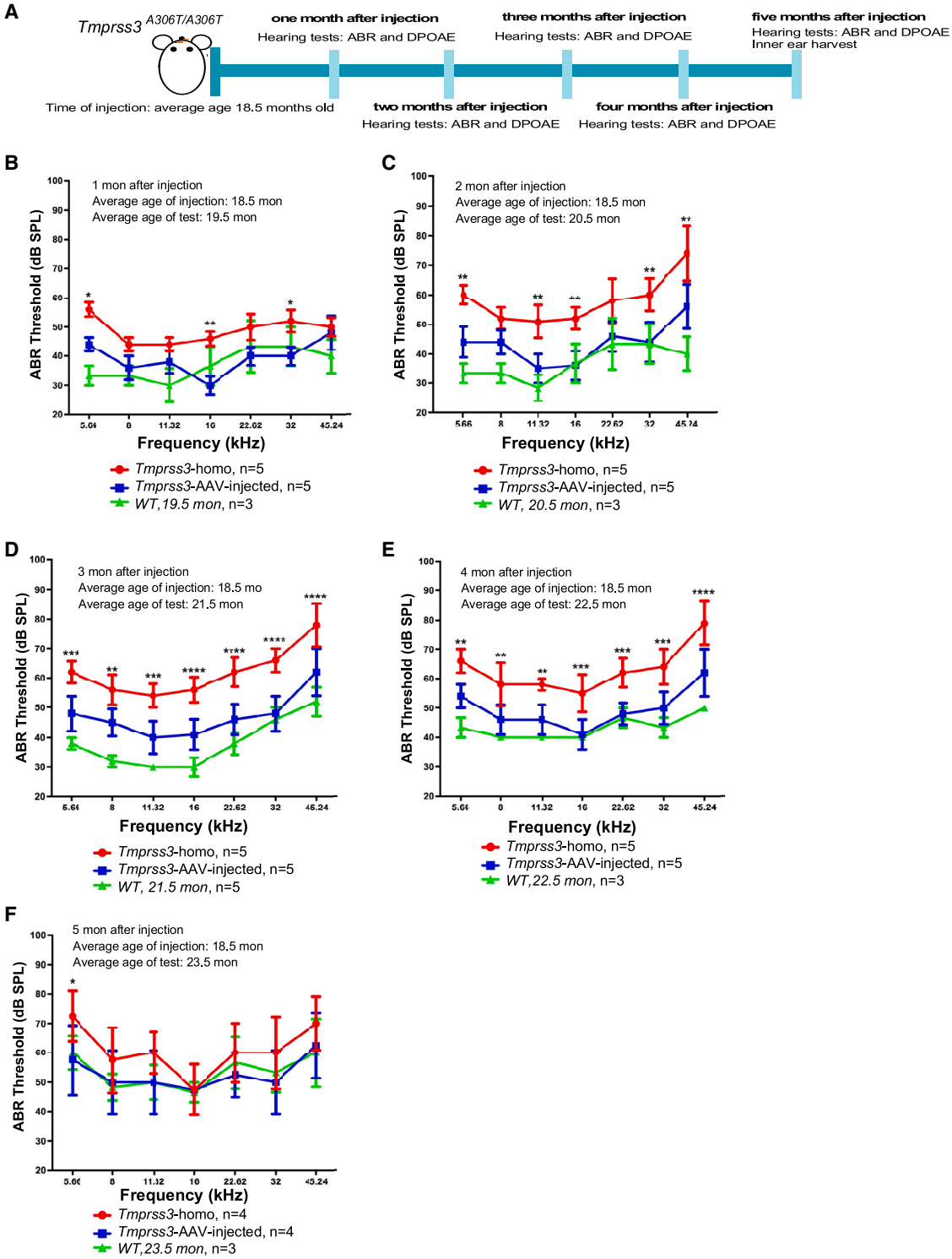

Figure 5. AAV2-h*TMPRSS3* injection in *Tmprss3*$^{A306T/A306T}$ mice rescues auditory function

(A) The schematic diagram of the experimental design. (B–F) ABR thresholds in *Tmprss3*$^{A306T/A306T}$ homozygous mice treated with AAV2-h*TMPRSS3* ears (blue), untreated *Tmprss3*$^{A306T/A306T}$ homozygous ears (red), and WT CBA/CaJ mice (green) at 1 month after injection (B), 2 months after injection (C), 3 months after injection (D), 4 months after injection (E), and 5 months after injection (F), respectively. Significant hearing rescue was detected at all time points with the exception at 5 months post injection when WT CBA/CaJ mice started to exhibit hearing loss. Values and error bars reflect mean ± SEM.

and 32 kHz (Figure 5B). For frequencies below 45.42 kHz, the ABR threshold reduction ranged from 6 dB at 11.32 kHz to 16 dB at 16 kHz, with an average reduction of 11 dB. No difference of DPOAE thresholds were detected between injected and uninjected ears (Figure S3B). The wave 1 amplitudes were statistically larger at 32 kHz above 50 dB SPL (Figure S3G). Two months after injection, ABR thresholds were further reduced at all frequencies in injected ears compared with uninjected control ears, ranging from 8 dB at 8 kHz to 18 dB at 45.24 kHz, with an average reduction of 15 dB across all frequencies (Figure 5C). Generally lower DPOAE thresholds were detected in injected compared with uninjected ears, with a significant reduction of 18 dB at 45.24 kHz (Figure S3C). At 3 and 4 months after injection, significant reductions in ABR thresholds were persistent in all frequencies in injected ears (Figures 5D and 5E), with an average reduction of 15 and 14 dB at 3 and 4 months, respectively. At the two time points, the DPOAE thresholds were generally lower and the wave 1 amplitudes at 32 kHz were larger in injected ears than in uninjected control ears (Figures S3D, S3E, 3I, and 3J). By 5 months post injection, with the exception of 16 kHz, ABR thresholds were still lower by an average of 9 dB (Figure 5F). Significant reduction in the DPOAE thresholds was detected at 8, 11.32, and 45.24 kHz (Figure S3F), and larger but not significant wave 1 amplitudes (Figure S3K) were seen in injected ears. At this age, the ABR thresholds in injected ears were indistinguishable from that of WT background CBA/CaJ strain at a comparable age of 23.5 months, which was elevated from that of CBA/CaJ of 22.5 months of age, an indication of ARHL in the CBA/CaJ background strain. In hearing tests of all ages, there was no significant difference of ABR thresholds between injected and WT CBA/CaJ ears (Figures 5B–5F), a demonstration of robust rescue of hearing by AAV2-h*TMPRSS3* delivery in the *Tmprss3*$^{A306T/A306T}$ ears to a level similar to that in the WT control ears. Based on the data we conclude that a single administration of gene therapy by AAV2-h*TMPRSS3* results in long-term hearing rescue in the *Tmprss3*$^{A306T/A306T}$ ears.

AAV2-h*TMPRSS3* promotes HC and SGN survival in *Tmprss3*$^{A306T/A306T}$ mice

Expression of *Tmprss3* in HC and SGN suggests the requirement of TMPRSS3 in HC and SGN . To study the effect of the *TMPRSS3* c.916G>A mutation on the inner ear and determine how AAV2-h*TMPRSS3* gene delivery rescued the cellular phenotype, we performed immunolabeling of injected and uninjected cochleae and quantified IHCs, OHCs, and SGN . In uninjected *Tmprss3*$^{A306T/A306T}$ inner ear, a loss of OHCs in the basal and middle regions was detected (Figures 6A1–A3). In contrast, in injected *Tmprss3*$^{A306T/A306T}$ ear, more OHCs survived in the same regions (Figures 6B1–B3 and 6C). No significant difference was detected in IHC number between injected and uninjected control ear, although the IHC average was higher in the injected ear (Figures 6A1–B3 and 6D). In the base to mid-base turns of the modiolus region of uninjected *Tmprss3*$^{A306T/A306T}$ ear, the TuJ1 labeling was condensed and localized to one side of the SGN (Figures 6E1 and 6E2). In contrast, evenly distributed cytoplasmic labeling of TuJ1 was detected in the SGN of injected ears (Figures 6F1 and 6F2). Significantly, 3-fold more SGN were detected in the injected ear compared with the uninjected ear (Figure 6G). Taken together, these results demonstrate that the *TMPRSS3* c.916G>A mutation caused the loss of the OHCs and SGN from base to mid-base at age 20.5 months and AAV2-h*TMPRSS3* gene therapy rescued hair cell and SGN in the same regions.

DISCUSSION

With the goal to develop gene therapy for DFNB8 in humans, we created a KI mouse model with a frequent human DFNB8 *TMPRSS3* mutation that exhibits late onset and progressive HL similar to DFNB5 patients. We show that one-time local administration of AAV2-h*TMPRSS3* gene therapy in aged KI mice of 18.5 months restores hearing at around age 2 years. Gene replacement therapy with the human *TMPRSS3* promotes the survival of HC and SGNs, both of which are required for hearing and the latter is essential to the treatment outcome of cochlear implants.

TMPRSS3 is a type II membrane serine protease and is associated with cancer development.[53,54] *Tmprss3* has been found to be expressed in the developing cochlea including HC and SGN .[55] The lack of TMPRSS3 has resulted in hair cell death in mouse organoids and SGN degeneration *in vitro*.[56,57] Patients with homozygous *TMPRSS3* mutations manifest either postlingual progressive HL (DFNB8) or congenital profound HL (DFNB10) (https://hereditaryhearingloss.org/recessive-genes),[39,58] likely due to the nature of the mutations. In *TMPRSS3* patients, cochlear implant is a standard form of treatment. Recently it has been suggested that, in some *TMPRSS3* patients, the treatment outcome may diminish over time, leaving the patients without any treatment option.[59,60] We aim to develop a gene therapy strategy to rescue hearing using a *TMPRSS3* mouse model with the potential to be further developed for the clinic.

AAV is one of the most effective gene delivery vectors that transduce both dividing and non-dividing cells to provide long-term gene expression.[61] In the inner ear, previous studies found that conventional AAVs could efficiently transduce IHCs but were less efficient in transducing OHCs.[31,32] We previously reported that AAV2 harboring GFP transduces almost all the IHCs and a large number of OHCs in adult C57BL/6 mouse cochleae by canalostomy.[62] This delivery route was also used in CBA/CaJ mouse cochleae to show efficient IHC and OHC transduction.[63] In a recent study, it was demonstrated that AAV2 transgene expression is in both OHCs (84%) and IHCs (97%) in adult C3H/FeJ mouse cochleae using a round window membrane plus canal fenestration delivery method.[64] Combined, these studies have indicated that animal strain, animal age, viral titer, viral promoter, and even viral processing and purifying procedure can affect transduction efficiency.[52,65] In this study, the human *TMPRSS3* gene was delivered into a mouse model by AAV2 in CBA/CaJ background using a round window membrane with canal fenestration delivery route, which showed robust transduction of IHCs and efficient transduction of OHCs.

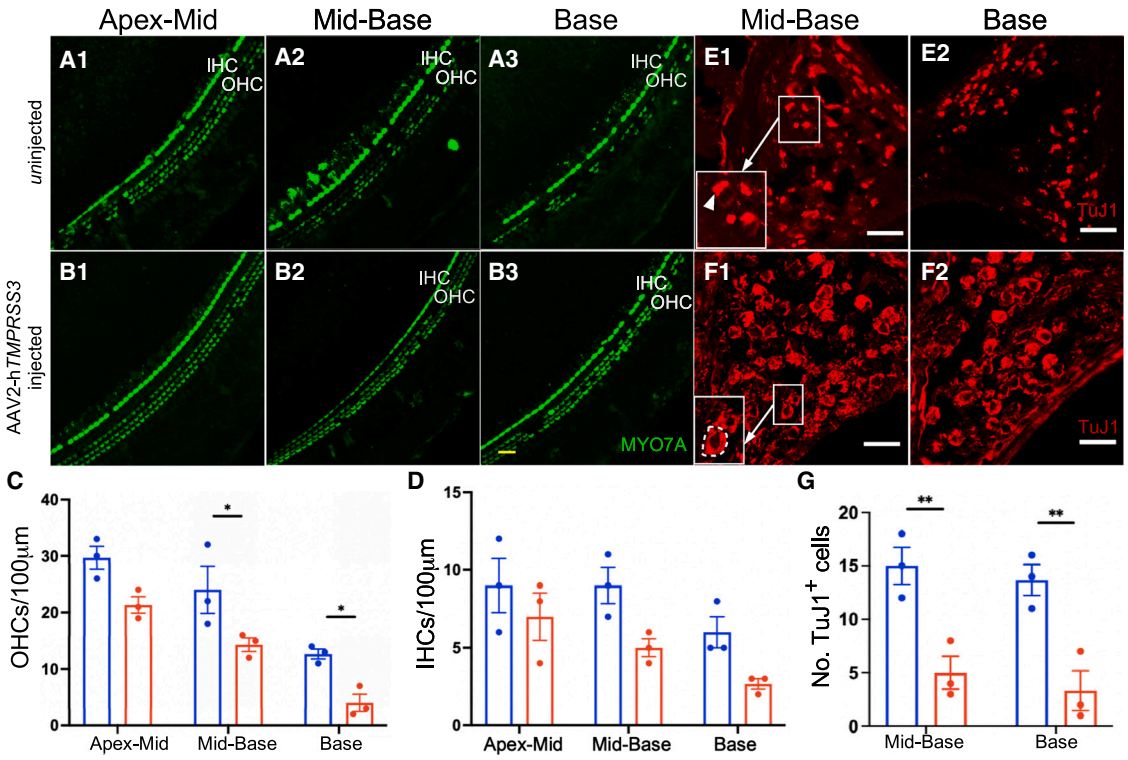

Figure 6. AAV2-h*TMPRSS3* injection rescues HC and SGN in *Tmprss3*$^{A306T/A306T}$ cochleae

(A and B) Representative confocal images of cochleae from uninjected (A) and AAV2-h*TMPRSS3*-injected (B) ears of *Tmprss3*$^{A306T/A306T}$ mouse at age 82 weeks. The apex-middle (A1, B1), middle-base (A2, B2), and base (A3, B3) turns were dissected and stained with MYO7A (green) for HC. (C and D) Quantification and comparison of OHCs (C) and IHCs (D) in three representative regions of apex-middle, middle-base, and base of injected (blue) and uninjected (red) *Tmprss3*$^{A306T/A306T}$ cochleae. Significantly more OHC survived in injected ear compared with uninjected ear in the base and middle-base turns. (E and F) Representative confocal images of a modiolus cross-section through the whole cochlea from uninjected (E) and AAV2-h*TMPRSS3*-injected (F) ear of *Tmprss3*$^{A306T/A306T}$ mouse at age 82 weeks. The middle-base modiolus (E1, F1) and base modiolus (E2, F2) were stained with TuJ1 (red) for the SGN . Arrows point to enlarged insets with higher magnifications of the square. Dotted circles showed an example of a SGN soma with TuJ1 labeling, with condensed TuJ1 labeling (arrowhead) localized to one side within an SGN in an uninjected ear (arrow). (G) Quantification and comparison of TuJ1-positive SGNs between uninjected (red) and AAV2-h*TMPRSS3*-injected (blue) *Tmprss3*$^{A306T/A306T}$ cochleae. Values and error bars reflect mean ± SEM. n = 3. Scale bars, 25 μm.

Gene therapy has been extensively used to treat mouse models for human genetic HL with success.[13,19,25,26,33,66] A majority of inner ear gene therapies, however, were only successful when performed in neonatal or young inner ears, not in adults.[13,23] This could be due to the fact that many types of genetic HL are congenital and the inner ear cell types to be targeted are severely damaged or no longer available when mature, thus limiting the efficacy by intervention in the mature inner ear. Furthermore, the delivery vehicles may show differences targeting neonatal or adult cochlear cell types.[10,62,67] In humans, even newborn inner ears are fully mature, so any gene therapy strategy for patients would require establishment of a window of opportunity for treatment and demonstration that successful hearing rescue can be achieved in fully mature animal inner ears. The *Tmprss3* knockout mouse exhibits severe congenital hair cell loss and profound HL,[39] and therefore is not a suitable model to develop *TMPRSS3* gene therapy to rescue hearing in the mature inner ear. We chose to create a mouse model with a frequent founder human *TMPRSS3* mutation c.916G>A (p.A306T) that causes postlingual progressive HL of DFNB8 in patients.[42,44] To circumvent the mouse inbred strains such as C57 with accelerated ARHL, we chose to use CBA/CaJ as the background strain, so that the strain-dependent HL is not manifested until an advanced age, which allowed us to study late onset progressive HL and the treatment outcome in aged mice. The combination of mutation and mouse strain selections are important factors that enabled us to establish a KI mouse model of DFNB8 that is progressive HL. The model is ideal to test our gene therapy strategy to rescue hearing in not only mature but aged inner ear by one-time AAV administration.

It is surprising that the delivery of the mouse WT *Tmprss3* copy into normal adult mouse HC leads to severe hair cell loss and profound HL. While the mechanism is not understood, it is likely that the level of the mouse TMPRSS3 protein is important to the survival of HC and essential for normal hearing. The detrimental effect of the mouse TMPRSS3 on HC and hearing prompted us to test the human *TMPRSS3* gene. Again, it is to our surprise that the human

TMPRSS3, despite sharing a high degree of homology with the mouse TMPRSS3, 88% identical on the protein sequence (Figure S4),[68] does not cause hair cell loss or HL. Given our goal of using the human *TMPRSS3* gene for the clinical development, we have thus chosen the human *TMPRSS3* for gene therapy intervention in the KI *Tmprss3* mouse model.

Due to the lack of a suitable anti-TMPRSS3 antibody, we carried out RNA-FISH (RNAscope) to study endogenous *Tmprss3* expression in mouse inner ear and evaluate the inner ear cells targeted by AAV2-hTMPRSS3. In the mouse, *Tmprss3* has been shown to be expressed in HC and other cochlear cell types including the cells in the modiolus region during development.[39,58] A recent study also showed low *TMPRSS3* expression in human auditory neurons.[58]

By RNAscope, we found that AAV2 carrying the human *TMPRSS3* CDS can properly target IHCs, OHCs, and SGNs. The *TMPRSS3* transgene expression pattern resembles that of the WT *Tmprss3* expression. The data strongly support our approach of AAV2 delivery in the mouse inner ear to target the cells that are directly affected by the lack of *Tmprss3* expression and evaluate the rescue effect. A few studies have reported that the outcomes of CI patients with *TMPRSS3*-related HL were inconsistent.[40,43,59,60,69,70] Our results could provide a promising therapeutic avenue for those patients who have poor CI outcomes.

The mouse inner ear still undergoes development until the onset of hearing at around P12.[71] However, in the clinic, it is impractical to perform genetic therapies at the corresponding ages in humans as the intervention would have to be carried out *in utero*. To translate these findings of preclinical mouse studies to humans, gene therapy research imperatively needs to focus on practical therapeutic strategies to perform in adult and aged mice. Among successful hearing rescue in animal models by gene or editing therapy, the vast majority of studies were carried out in the neonatal or infant stage.[13–17,19,21–25,29,32,35,72,73] In $Tmprss3^{A306T/A306T}$ mice, HL does not start until age ~16.5 months, thus the intervention in aged mouse inner ears would be ideal to determine the treatment effect. We started injection in the animals of an average age of 18.5 months and measured hearing 1 month after injection and continued the testing monthly for 5 months. Significant hearing rescue by the reduction in the ABR thresholds was detected 1 month after injection at some frequencies (Figure 5B). The rescue effect extended to all frequencies with increasing magnitudes (Figures 5C–5E). Overall, there is a decrease in average DPOAE thresholds and greater wave 1 amplitudes in injected compared with uninjected contralateral control $Tmprss3^{A306T/A306T}$ ears (Figure S3), supporting the improved OHC function and neuronal activities. The improved hearing was detected 4 months after injection at an age of 22.5 months. At 5 months post injection with average age of mice at 23.5 months, even the WT control mice of the same age started to exhibit ARHL, with an ABR threshold average that was indistinguishable from injected $TMPRSS3^{A306T/A306T}$mice (Figure 5F). We conclude that the strain-specific ARHL obscured the treatment effect by AAV2-h*TMPRSS3* injection at 23.5 months. Our study demonstrates that one-time administration of AAV gene therapy in aged mice is sufficient to rescue hearing long term in mice due to a *TMPRSS3* A306T mutation. The *TMPRSS3* A306T is a common mutation that has been described in German, Dutch, Korean, and Chinese families.[40–44] While our gene therapy has shown efficacy in treating the $Tmprss3^{A306T/A306T}$ mouse model, the same AAV2-h*TMPRSS3* is applicable to all DFNB8 patients with *TMPRSS3* mutations. Hearing rescue by local injection at an advanced age in mice offers a wide therapeutic window that could enable the intervention in patients with DFNB8.

In the $Tmprss3^{A306T/A306T}$ mice, significant hair cell, especially OHC, and neuronal loss was detected (Figure 6). In contrast to the *Tmprss3* knockout mice in which HC die rapidly,[39] our model with the A306T mutation showed a gradual hair cell and neuronal loss, which is consistent with late onset and progressive HL. After AAV2-h*TMPRSS3* injection, both cell types survived significantly better, which is consistent with those cells targeted by AAV2. Interestingly, we also observed that TuJ1, a neuronal marker, showed an aggregation-like pattern with condensed TuJ1 signal restricted to neuron cell bodies unilaterally in the $Tmprss3^{A306T/A306T}$ mice, which may further support previous findings showing cellular and molecular basis of SGN degeneration and the subsequent decline of the auditory nerve function in presbyacusis.[74] While the physiological outcomes of TuJ1 aggregation is unknown, both the altered TuJ1 localization and the neuronal loss strongly support the direct impact of the *TMPRSS3* mutation A306T on the SGN and the rescue effect by AAV2-h*TMPRSS3* local delivery. Mutations in *TMPRSS3* cause DFNB8 with HL that is postlingual and progressive, and DFNB10 with congenital profound HL. For DFNB8 patients, it is highly likely that HC and SGNs are present after birth, and they degenerate overtime. For DFNB8 patients, early intervention by AAV2-h*TMPRSS3* gene therapy may be used as a standalone therapy to rescue HC and SGNs to prevent HL. For *TMPRSS3* patients with profound HL, their HC may have severely degenerated, and CI is the only option for treatment. For those patients, AAV2-h*TMPRSS3* gene delivery can be used to promote SGN survival to enhance long-term CI treatment outcomes. In addition to HL caused by homozygous or compound heterozygous *TMPRSS3* mutations, there has been an increase in reports that heterozygous *TMPRSS3* mutations could contribute to accelerated ARHL[75] in conjunction with a compound heterozygous mutation in another deafness gene.[76,77] It is thus conceivable that gene therapy for *TMPRSS3* developed in this study could be expanded to rescue hearing in a subset of patients exhibiting ARHL with the contribution of *TMPRSS3* mutations. The study supports that a single administration of AAV gene therapy for *TMPRSS3* in fully mature and aged inner ears could achieve noticeable restoration of hearing with long-term therapeutic effect. It is the proof-of-principle demonstration that gene therapy could be successfully implemented at a late stage in life and builds a solid foundation for its future clinical application.

MATERIALS AND METHODS

Animals

Tmprss3$^{A306T/A306T}$ mutant mice were generated at the Mouse Genome Engineering Core Facility of University of Nebraska Medical Center. The background was CBA/CaJ strain (Jackson Laboratory stock no. 000656) to eliminate the effect of ARHL. The mice were housed in groups of two to five per cage and allowed free access to food and water. The animals were maintained under standard conditions (room temperature [RT]: 22°C ± 2°C; relative humidity: 55% ± 10%) on a light:dark cycle of 12:12 h (6:00 a.m. to 6:00 p.m.). All procedures were approved by the Massachusetts Eye & Ear IACUC committee (protocol no. 08-04-008) and University of Miami Institutional Animal Care Committee (protocol no. 19–104), following the National Institutes of Health (NIH) Guidelines. All mouse experiments were performed in accordance with NIH guidelines for use and care of laboratory animals and were approved by the Massachusetts Eye & Ear IACUC committee (protocol no. 08-04-008).

Recombinant DNA constructs and AAV virus production

To construct recombinant AAV2 plasmids, CDSs for human *TMPRSS3* (GenBank: accession no. BC074846; CDS: 1,362 bp, 453 aa) and mouse *Tmprss3* (Genbank: accession no. NM_001163776; CDS: 1,428 bp, 475 aa) were individually inserted in the host vector linearized by NotI and BamHI enzymes. CDSs amplified by PCR were subcloned downstream of the hCMV enhancer/promoter in the host vector via In-Fusion HD enzyme (Takara), which fuses PCR-generated amplicons and linearized vector precisely by recognizing a 15 bp overlap at their ends. All constructs were sequenced prior to transfections to ensure no mutations were introduced during cloning. All the plasmids were propagated in DH5a *E. coli* cells and plasmids were extracted using endo-free plasmid purification kits (QIAGEN).

For recombinant AAV production, transgene vectors were packaged at the University of Massachusetts Medical School, Viral Vector Core, as described previously.[78] In brief, HEK293 cells maintained in DMEM with GlutaMAX, penicillin/streptomycin, and 10% FBS were co-transfected with packaging plasmid (pRep2/Cap2; Agilent Technologies), adenovirus helper plasmid (pHelper; Agilent Technologies), and rAAV plasmid carrying a human or mouse full-length Tmprss3 expression cassette flanked by AAV2 ITRs. The pRep2/Cap2 expresses regulatory and capsid proteins of AAV2 serotype, which excises the recombinant genome from the rAAV vector plasmid, replicates the viral ssDNA genome, and packages the genome into AAV virions. Adenovirus E2A, E4, and viral-associated RNAs expressed from the pHelper provide helper functions essential for rAAV rescue, replication, and packaging.[79] HEK293 cells were harvested 72 h post-transfection, suspended in a lysis buffer containing 50 mM Tris-HCl (pH 8.0), 150 mM NaCl, and 1 mM $MgCl_2$, and lysed by three freeze-thaw cycles. Unencapsidated plasmid DNA was digested using 250 U Benzonase (Sigma-Aldrich), and virions were purified by ultracentrifugation on standard CsCl gradient and desalted by dialysis. The vectors are quality control tested by ddPCR titration for DNase-resistant vector genome concentration using probe and primers targeting the bGH region, and AAV purity was assessed by 4%–12% SDS-acrylamide gel electrophoresis followed by silver staining (Invitrogen). Viral genomic titers for AAV2.CMV.h*TMPRSS3* and AAV2.CMV.m*Tmprss3* were calculated as 1.1 × 10E-13 and 1.0 × 10E-13 GC/mL, respectively.

ANIMAL SURGERY

Tmprss3$^{A306T/A306T}$ and WT mice of either sex were anesthetized using intraperitoneal injection of ketamine (100 mg/kg) and xylazine (10 mg/kg). The post-auricular incision was exposed by shaving and disinfected using 10% povidone iodine. The AAV2-m*Tmprss3* and AAV2-h*TMPRSS3* were injected into the inner ears of WT and *Tmprss3*$^{A306T/A306T}$ mice. The AAV2-GFP was injected into the inner ears of WT mice. The total volume for each injection was 1 μL virus per cochlea.

Auditory brainstem response and DPOAE

Mice of either sex were anesthetized under the same conditions as for surgery. For ABR measurements, subcutaneous needle electrodes were inserted at the vertex (reference), ventral edge of the pinna (active electrode), and a ground reference near the tail. In a soundproof chamber, mice were presented with 5-ms tone pips (delivered at 35/s). The response was amplified 10,000-fold, then filtered (100 Hz–3 kHz band-pass), digitized, and averaged (1,024 responses) at each SPL. The sound level was elevated in 5-dB steps from 20 up to 90 dB SPL at stimuli of 5.66–45.24 kHz frequencies (in half-octave steps). The threshold and wave 1 amplitude were identified as described previously.[17] During the same recording session, DPOAEs were measured under the same conditions as for ABRs. In brief, two primary tones (f2/f1 = 1.2) were set, with f2 varied between 5.66 and 45.24 kHz in half-octave steps. Primaries were swept from 20 to 80 dB SPL (for f2) in 5-dB steps. Thresholds required to produce a DPOAE at 5 dB SPL were computed by interpolation as f2 level. The information on the animals studied including the age of injection, the age of hearing tests, and the age of inner ear harvest is provided in Table S1.

Confocal microscopy and cell counting

Injected and uninjected cochleae were harvested from mice euthanized by CO_2 inhalation. Temporal bones were fixed in 4% paraformaldehyde at 4°C overnight, then decalcified in 120 mM EDTA for at least 7 days until the tissues softened. After decalcification, the cochleae were dissected for whole-mount immunostaining or cryosection at 10 μm thickness using published methods.[17,80,81] Tissues were infiltrated with 0.25% Triton X-100 and blocked with donkey serum (5%) for 1 h at RT, followed by washing 3 × 10 min with PBS and then incubated with primary antibody. Rabbit anti-MYO7A (1:500; Proteus BioSciences, no. 25-6790), mouse anti-beta III tubulin (1:250; BioLegend, no. 801201), and chicken anti-GFP (1:1000; Abcam, ab13970) were used overnight. Tissues were then washed for 3 × 10 min with PBS and the secondary antibodies were incubated for 1 h (donkey anti-rabbit IgG Alexa Fluor Plus 488, 1:1,000; donkey anti-mouse IgG Alexa Fluor Plus 594, 1:1,000;

Thermo Fisher Scientific). Following secondary antibody incubation, tissues were washed for 3 × 10 min with PBS. Finally, tissues were placed on a microscope slide and mounted with VECTASHIELD antifade mounting medium containing DAPI (Vector Laboratories, no. H-1200). Images were taken with a Leica SP8 confocal laser scanning microscope (Leica Microsystems, Germany) via a 20× or 63× glycerin immersion lens. Images were edited by ImageJ software and tools in ImageJ were used for counting of HC and SGNs. For hair cell counting, Myosin7a-positive HC per 100 μm length were calculated in the apical, middle, and basal turns of cochleae. We counted at least two 100-μm segments from at least three independent cochleae. For SGN cell counting, TUJ1-positive cells were calculated in the SGN area. The average cell number per 10^4 μm^2 was calculated for data analysis.

RNA-FISH, immunohistochemistry, and data quantification

RNA-FISH was performed using an RNAscope Multiplex Fluorescent Reagent Kit v.2 (ACD, no. 323110), and the protocol described here is adapted from Huang and Eckrich[50,51] with minor modifications.[50,51] In brief, membranous labyrinths were removed, and cochleae were immediately soaked in ice-cold 4% PFA in PBS. Cochleae were fixed for 2 h at RT on a shaker and washed for 3 × 10 min in 0.1% Tween 20 in PBS (PBT20), and subsequently dehydrated in a graded MeOH series (50%, 75%, and 100% in PBT20, 10 min for each grade). At the same time, probes were pre-warmed to 40°C for 10 min to allow aggregates to dissolve and then cooled down to RT. Protease III solution and Amplifiers I-IV were allowed to equilibrate to RT.

Before hybridization, cochleae were rehydrated at RT in a reverse MeOH series (100%, 75%, and 50% in PBT20; 10 min for each grade) and washed 6 × 5 min in PBT20. During the last washing step, the apical turn was dissected in PBT20 in a 35-mm sterile dish, and the stria vascularis and spiral ligament were carefully removed. Reissner's membrane and the tectorial membrane were also separated from the sensory epithelium with fine forceps while the SGN was maintained intact. Dissected tissues collected from different sample groups were placed in individual mini cell strainers (pluriStrainer Mini 40 μm) containing 1 mL of PBT20, which were then transferred manually between the wells of a 24-well plate during all incubation and washing steps.

Dissected cochlea pieces were digested for 12 min at RT in 300 mL of Protease III solution. Following washing with 1 mL of PBT20 for 6 × 5 min to remove residual proteases, samples were incubated with hybridization probes for 2 h at 40°C. We used target probes against mouse *TMPRSS3* mRNA (ACD, no. 553861) or human *TMPRSS3* mRNA (ACD, no. 524691-C2). Subsequently, tissues were washed for 6 × 5 min with 1 mL of ACD washing buffer, re-fixed for 10 min with 4% PFA, and washed again for 6 × 5 min. Probe signals were amplified by incubation at 40°C in 4–5 drops of Amp1 (35 min), Amp2 (20 min), Amp3 (35 min), and Amp4 "Alt-A″" solution (20 min), respectively. Following each step, tissues were washed for 6 × 5 min in 1 mL of ACD washing buffer in mini cell strainers housed in a 24-well plate.

For a more precise identification of different cell types, the RNAscope assay was coupled to immunohistochemistry. In brief, tissues were permeabilized for 10 min with 0.5% Triton X-100 in PBS (PBST), and blocked for 1 h with 10% donkey serum in PBST at RT. Subsequently, samples were incubated with primary antibodies against MYO7A (polyclonal rabbit, 1:250, Proteus Biosciences, no. 25-6790) and HuD (monoclonal mouse, 1:100, SantaCruz, no. sc-48421) in antibody incubation buffer (5% donkey serum and 0.25% PBST) for 1 h at RT. Following washing with 0.1% PBST for 3 × 5 min, tissues were incubated at RT for 1 h with appropriate secondary antibodies (donkey α-rabbit IgG Alexa Fluor Plus 594, 1:500; donkey α-mouse IgG Alexa Fluor Plus 647, 1:500; Thermo Fisher Scientific) in the antibody incubation buffer. Following secondary antibody incubation, tissues were washed for 3 × 5 min with 0.1% PBST. Finally, tissues were placed on a microscope slide and mounted with Prolong Gold DAPI antifade medium (Invitrogen, no. P36931), and allowed to penetrate and solidify overnight before imaging.

RNAscope plus immunohistochemistry experiments were repeated in more than two animals per group. For each sample group, ≥5 z stack images were acquired using a 63× oil objective with 2× digital zoom in a Leica SP8 confocal laser scanning microscope. Fluorescently labeled mRNA was quantified using the particle analysis tool in ImageJ, which requires 8-bit grayscale images. After adjusting thresholds to remove background signal for each image, the average number of mRNA molecules per hair cell was determined by dividing the number of particles by the number of MYO7A-positive HC or by the total number of particles per HuD-positive SGN . For counting of IHCs, OHCs, and SGNs, we acquired z stacks by maximum intensity projections. The average number of IHCs and OHCs per hair cell was determined by dividing the number of particles by the number of MYO7A-positive HC or by the total number of particles per HuD-positive SGN .

Statistical analysis

We used GraphPad Prism (v.9, GraphPad Software, La Jolla, CA) for statistical analysis. For multiple comparisons in terms of ABRs and DPOAEs, statistical analyses were carried out by two-way ANOVA with Bonferroni corrections. For a numeric representation of RNAscope data, scatter column graphs were created using five z stack images. For comparisons between two groups, data were analyzed by two-tailed unpaired t tests with Welch's correction. Significance threshold was set as $p < 0.05$ (*$p < 0.05$, **$p < 0.01$, ***$p < 0.001$, ****$p < 0.0001$).

DATA AVAILABILITY

All study data are included in the article and/or supplemental information.

SUPPLEMENTAL INFORMATION

Supplemental information can be found online at https://doi.org/10.1016/j.ymthe.2023.05.005.

ACKNOWLEDGMENTS

This work was supported by NIH R01DC016875, UG3TR002636, and UH3TR002636 (to Z.-Y.C.), R01DC019404 (to X.L. and Z.-Y.C.), Ines-Fredrick Yeatts Fund (to Z.-Y.C.), R01DC012115, R01DC005575, and DOD RH220053 (to X.L.). We acknowledge the BioRender that was used to create the graphical abstract. We acknowledge Olivia Catalini for help with the illustration.

AUTHOR CONTRIBUTIONS

H.S., X.L., and Z.-Y.C. supervised the project. W.D., V.E., H.S., X.L., and Z.-Y.C. designed the experiments. W.D., V.E., C.L., M.H., S.S., A.M.A., Z.H., C.B.G., and H.S. conducted the experiments. All authors analyzed data. W.D., V.E., C.L., and Z.-Y.C. wrote the manuscript. All authors reviewed and edited the manuscript.

DECLARATION OF INTERESTS

Z.-Y.C. is a co-founder and a SAB member of Salubritas Therapeutics. X.L. and H.S. are scientific advisors to Rescue Hearing Inc.

REFERENCES

1. World Health Organization (2020). Deafness and hearing loss. https://www.who.int/news-room/fact-sheets/detail/deafness-and-hearing-loss.
2. Lin, F.R., Yaffe, K., Xia, J., Xue, Q.L., Harris, T.B., Purchase-Helzner, E., Satterfield, S., Ayonayon, H.N., Ferrucci, L., and Simonsick, E.M.; Health ABC Study Group (2013). Hearing loss and cognitive decline in older adults. JAMA Intern. Med. *173*, 293–299.
3. Thomson, R.S., Auduong, P., Miller, A.T., and Gurgel, R.K. (2017). Hearing loss as a risk factor for dementia: a systematic review. Laryngoscope Investig. Otolaryngol. *2*, 69–79.
4. Géléoc, G.S.G., and Holt, J.R. (2014). Sound strategies for hearing restoration. Science *344*, 1241062.
5. Müller, U., and Barr-Gillespie, P.G. (2015). New treatment options for hearing loss. Nat. Rev. Drug Discov. *14*, 346–365.
6. Lenz, D.R., and Avraham, K.B. (2011). Hereditary hearing loss: from human mutation to mechanism. Hear. Res. *281*, 3–10.
7. Shearer, A.E., Hildebrand, M.S., Sloan, C.M., and Smith, R.J.H. (2011). Deafness in the genomics era. Hear. Res. *282*, 1–9.
8. Lin, X., Tang, W., Ahmad, S., Lu, J., Colby, C.C., Zhu, J., and Yu, Q. (2012). Applications of targeted gene capture and next-generation sequencing technologies in studies of human deafness and other genetic disabilities. Hear. Res. *288*, 67–76.
9. Pillay, S., Zou, W., Cheng, F., Puschnik, A.S., Meyer, N.L., Ganaie, S.S., Deng, X., Wosen, J.E., Davulcu, O., Yan, Z., et al. (2017). Adeno-associated virus (AAV) serotypes have distinctive interactions with domains of the cellular AAV receptor. J. Virol. *91*, e00391-17.
10. Landegger, L.D., Pan, B., Askew, C., Wassmer, S.J., Gluck, S.D., Galvin, A., Taylor, R., Forge, A., Stankovic, K.M., Holt, J.R., and Vandenberghe, L.H. (2017). A synthetic AAV vector enables safe and efficient gene transfer to the mammalian inner ear. Nat. Biotechnol. *35*, 280–284.
11. Russell, S., Bennett, J., Wellman, J.A., Chung, D.C., Yu, Z.F., Tillman, A., Wittes, J., Pappas, J., Elci, O., McCague, S., et al. (2017). Efficacy and safety of voretigene neparvovec (AAV2-hRPE65v2) in patients with RPE65-mediated inherited retinal dystrophy: a randomised, controlled, open-label, phase 3 trial. Lancet *390*, 849–860.
12. Day, J.W., Finkel, R.S., Chiriboga, C.A., Connolly, A.M., Crawford, T.O., Darras, B.T., Iannaccone, S.T., Kuntz, N.L., Peña, L.D.M., Shieh, P.B., et al. (2021). Onasemnogene abeparvovec gene therapy for symptomatic infantile-onset spinal muscular atrophy in patients with two copies of SMN2 (STR1VE): an open-label, single-arm, multicentre, phase 3 trial. Lancet Neurol. *20*, 284–293.
13. Nist-Lund, C.A., Pan, B., Patterson, A., Asai, Y., Chen, T., Zhou, W., Zhu, H., Romero, S., Resnik, J., Polley, D.B., et al. (2019). Improved TMC1 gene therapy restores hearing and balance in mice with genetic inner ear disorders. Nat. Commun. *10*, 236.
14. Askew, C., Rochat, C., Pan, B., Asai, Y., Ahmed, H., Child, E., Schneider, B.L., Aebischer, P., and Holt, J.R. (2015). Tmc gene therapy restores auditory function in deaf mice. Sci. Transl. Med. *7*, 295ra108.
15. Yoshimura, H., Shibata, S.B., Ranum, P.T., Moteki, H., and Smith, R.J.H. (2019). Targeted allele suppression prevents progressive hearing loss in the mature murine model of human TMC1 deafness. Mol. Ther. *27*, 681–690.
16. Shibata, S.B., Ranum, P.T., Moteki, H., Pan, B., Goodwin, A.T., Goodman, S.S., Abbas, P.J., Holt, J.R., and Smith, R.J.H. (2016). RNA interference prevents autosomal-dominant hearing loss. Am. J. Hum. Genet. *98*, 1101–1113.
17. Gao, X., Tao, Y., Lamas, V., Huang, M., Yeh, W.H., Pan, B., Hu, Y.J., Hu, J.H., Thompson, D.B., Shu, Y., et al. (2018). Treatment of autosomal dominant hearing loss by in vivo delivery of genome editing agents. Nature *553*, 217–221.
18. György, B., Meijer, E.J., Ivanchenko, M.V., Tenneson, K., Emond, F., Hanlon, K.S., Indzhykulian, A.A., Volak, A., Karavitaki, K.D., Tamvakologos, P.I., et al. (2019). Gene transfer with AAV9-PHP.B rescues hearing in a mouse model of Usher syndrome 3A and transduces hair cells in a nonhuman primate. Mol. Ther. Methods Clin. Dev. *13*, 1–13.
19. Dulon, D., Papal, S., Patni, P., Cortese, M., Vincent, P.F., Tertrais, M., Emptoz, A., Tlili, A., Bouleau, Y., Michel, V., et al. (2018). Clarin-1 gene transfer rescues auditory synaptopathy in model of Usher syndrome. J. Clin. Invest. *128*, 3382–3401.
20. Geng, R., Omar, A., Gopal, S.R., Chen, D.H.C., Stepanyan, R., Basch, M.L., Dinculescu, A., Furness, D.N., Saperstein, D., Hauswirth, W., et al. (2017). Modeling and preventing progressive hearing loss in Usher syndrome III. Sci. Rep. *7*, 13480.
21. Pan, B., Askew, C., Galvin, A., Heman-Ackah, S., Asai, Y., Indzhykulian, A.A., Jodelka, F.M., Hastings, M.L., Lentz, J.J., Vandenberghe, L.H., et al. (2017). Gene therapy restores auditory and vestibular function in a mouse model of Usher syndrome type 1c. Nat. Biotechnol. *35*, 264–272.
22. Lentz, J.J., Jodelka, F.M., Hinrich, A.J., McCaffrey, K.E., Farris, H.E., Spalitta, M.J., Bazan, N.G., Duelli, D.M., Rigo, F., and Hastings, M.L. (2013). Rescue of hearing and vestibular function by antisense oligonucleotides in a mouse model of human deafness. Nat. Med. *19*, 345–350.
23. Chien, W.W., Isgrig, K., Roy, S., Belyantseva, I.A., Drummond, M.C., May, L.A., Fitzgerald, T.S., Friedman, T.B., and Cunningham, L.L. (2016). Gene therapy restores hair cell stereocilia morphology in inner ears of deaf whirler mice. Mol. Ther. *24*, 17–25.
24. Isgrig, K., Shteamer, J.W., Belyantseva, I.A., Drummond, M.C., Fitzgerald, T.S., Vijayakumar, S., Jones, S.M., Griffith, A.J., Friedman, T.B., Cunningham, L.L., and Chien, W.W. (2017). Gene therapy restores balance and auditory functions in a mouse model of Usher syndrome. Mol. Ther. *25*, 780–791.
25. Akil, O., Dyka, F., Calvet, C., Emptoz, A., Lahlou, G., Nouaille, S., Boutet de Monvel, J., Hardelin, J.P., Hauswirth, W.W., Avan, P., et al. (2019). Dual AAV-mediated gene therapy restores hearing in a DFNB9 mouse model. Proc. Natl. Acad. Sci. USA *116*, 4496–4501.
26. Al-Moyed, H., Cepeda, A.P., Jung, S., Moser, T., Kügler, S., and Reisinger, E. (2019). A dual-AAV approach restores fast exocytosis and partially rescues auditory function in deaf otoferlin knock-out mice. EMBO Mol. Med. *11*, e9396.
27. György, B., Sage, C., Indzhykulian, A.A., Scheffer, D.I., Brisson, A.R., Tan, S., Wu, X., Volak, A., Mu, D., Tamvakologos, P.I., et al. (2017). Rescue of hearing by gene delivery to inner ear hair cells using exosome-associated AAV. Mol. Ther. *25*, 379–391.
28. Kim, M.A., Cho, H.J., Bae, S.H., Lee, B., Oh, S.K., Kwon, T.J., Ryoo, Z.Y., Kim, H.Y., Cho, J.H., Kim, U.K., and Lee, K.Y. (2016). Methionine sulfoxide reductase B3-targeted in utero gene therapy rescues hearing function in a mouse model of congenital sensorineural hearing loss. Antioxid. Redox Signal. *24*, 590–602.
29. Chang, Q., Wang, J., Li, Q., Kim, Y., Zhou, B., Wang, Y., Li, H., and Lin, X. (2015). Virally mediated Kcnq1 gene replacement therapy in the immature scala media restores hearing in a mouse model of human Jervell and Lange-Nielsen deafness syndrome. EMBO Mol. Med. *7*, 1077–1086.
30. Iizuka, T., Kamiya, K., Gotoh, S., Sugitani, Y., Suzuki, M., Noda, T., Minowa, O., and Ikeda, K. (2015). Perinatal Gjb2 gene transfer rescues hearing in a mouse model of hereditary deafness. Hum. Mol. Genet. *24*, 3651–3661.

31. Yu, Q., Wang, Y., Chang, Q., Wang, J., Gong, S., Li, H., and Lin, X. (2014). Virally expressed connexin26 restores gap junction function in the cochlea of conditional Gjb2 knockout mice. Gene Ther. *21*, 71–80.

32. Akil, O., Seal, R.P., Burke, K., Wang, C., Alemi, A., During, M., Edwards, R.H., and Lustig, L.R. (2012). Restoration of hearing in the VGLUT3 knockout mouse using virally mediated gene therapy. Neuron *75*, 283–293.

33. Taiber, S., Cohen, R., Yizhar-Barnea, O., Sprinzak, D., Holt, J.R., and Avraham, K.B. (2021). Neonatal AAV gene therapy rescues hearing in a mouse model of SYNE4 deafness. EMBO Mol. Med. *13*, e13259.

34. Delmaghani, S., Defourny, J., Aghaie, A., Beurg, M., Dulon, D., Thelen, N., Perfettini, I., Zelles, T., Aller, M., Meyer, A., et al. (2015). Hypervulnerability to sound exposure through impaired adaptive proliferation of peroxisomes. Cell *163*, 894–906.

35. Emptoz, A., Michel, V., Lelli, A., Akil, O., Boutet de Monvel, J., Lahlou, G., Meyer, A., Dupont, T., Nouaille, S., Ey, E., et al. (2017). Local gene therapy durably restores vestibular function in a mouse model of Usher syndrome type 1G. Proc. Natl. Acad. Sci. USA *114*, 9695–9700.

36. Bademci, G., Foster, J., Mahdieh, N., Bonyadi, M., Duman, D., Cengiz, F.B., Menendez, I., Diaz-Horta, O., Shirkavand, A., Zeinali, S., et al. (2016). Comprehensive analysis via exome sequencing uncovers genetic etiology in autosomal recessive nonsyndromic deafness in a large multiethnic cohort. Genet. Med. *18*, 364–371.

37. Sloan-Heggen, C.M., Bierer, A.O., Shearer, A.E., Kolbe, D.L., Nishimura, C.J., Frees, K.L., Ephraim, S.S., Shibata, S.B., Booth, K.T., Campbell, C.A., et al. (2016). Comprehensive genetic testing in the clinical evaluation of 1119 patients with hearing loss. Hum. Genet. *135*, 441–450.

38. Scott, H.S., Kudoh, J., Wattenhofer, M., Shibuya, K., Berry, A., Chrast, R., Guipponi, M., Wang, J., Kawasaki, K., Asakawa, S., et al. (2001). Insertion of β-satellite repeats identifies a transmembrane protease causing both congenital and childhood onset autosomal recessive deafness. Nat. Genet. *27*, 59–63.

39. Fasquelle, L., Scott, H.S., Lenoir, M., Wang, J., Rebillard, G., Gaboyard, S., Venteo, S., François, F., Mausset-Bonnefont, A.L., Antonarakis, S.E., et al. (2011). Tmprss3, a transmembrane serine protease deficient in human DFNB8/10 deafness, is critical for cochlear hair cell survival at the onset of hearing. J. Biol. Chem. *286*, 17383–17397.

40. Weegerink, N.J.D., Schraders, M., Oostrik, J., Huygen, P.L.M., Strom, T.M., Granneman, S., Pennings, R.J.E., Venselaar, H., Hoefsloot, L.H., Elting, M., et al. (2011). Genotype-phenotype correlation in DFNB8/10 families with TMPRSS3 mutations. J. Assoc. Res. Otolaryngol. *12*, 753–766.

41. Lee, J., Baek, J.I., Choi, J.Y., Kim, U.K., Lee, S.H., and Lee, K.Y. (2013). Genetic analysis of TMPRSS3 gene in the Korean population with autosomal recessive nonsyndromic hearing loss. Gene *532*, 276–280.

42. Chung, J., Park, S.M., Chang, S.O., Chung, T., Lee, K.Y., Kim, A.R., Park, J.H., Kim, V., Park, W.Y., Oh, S.H., et al. (2014). A novel mutation of TMPRSS3 related to milder auditory phenotype in Korean postlingual deafness: a possible future implication for a personalized auditory rehabilitation. J. Mol. Med. *92*, 651–663.

43. Elbracht, M., Senderek, J., Eggermann, T., Thürmer, C., Park, J., Westhofen, M., and Zerres, K. (2007). Autosomal recessive postlingual hearing loss (DFNB8): compound heterozygosity for two novel TMPRSS3 mutations in German siblings. J. Med. Genet. *44*, e81.

44. Gao, X., Yuan, Y.Y., Wang, G.J., Xu, J.C., Su, Y., Lin, X., and Dai, P. (2017). Novel mutations and mutation combinations of TMPRSS3 cause various phenotypes in one Chinese family with autosomal recessive hearing impairment. Biomed. Res. Int. *2017*, 4707315.

45. Erway, L.C., Shiau, Y.W., Davis, R.R., and Krieg, E.F. (1996). Genetics of age-related hearing loss in mice. III. Susceptibility of inbred and F1 hybrid strains to noise-induced hearing loss. Hear. Res. *93*, 181–187.

46. Chen, X., Abad, C., Chen, Z.Y., Young, J.I., Gurumurthy, C.B., Walz, K., and Liu, X.Z. (2021). Generation and characterization of a P2rx2 V60L mouse model for DFNA41. Hum. Mol. Genet. *30*, 985–995.

47. Quadros, R.M., Miura, H., Harms, D.W., Akatsuka, H., Sato, T., Aida, T., Redder, R., Richardson, G.P., Inagaki, Y., Sakai, D., et al. (2017). Easi-CRISPR: a robust method for one-step generation of mice carrying conditional and insertion alleles using long ssDNA donors and CRISPR ribonucleoproteins. Genome Biol. *18*, 92.

48. Miura, H., Quadros, R.M., Gurumurthy, C.B., and Ohtsuka, M. (2018). Easi-CRISPR for creating knock-in and conditional knockout mouse models using long ssDNA donors. Nat. Protoc. *13*, 195–215.

49. Harms, D.W., Quadros, R.M., Seruggia, D., Ohtsuka, M., Takahashi, G., Montoliu, L., and Gurumurthy, C.B. (2014). Mouse genome editing using the CRISPR/Cas system. Curr. Protoc. Hum. Genet. *83*, 1–27.

50. Wang, F., Flanagan, J., Su, N., Wang, L.C., Bui, S., Nielson, A., Wu, X., Vo, H.T., Ma, X.J., and Luo, Y. (2012). RNAscope: a novel in situ RNA analysis platform for formalin-fixed, paraffin-embedded tissues. J. Mol. Diagn. *14*, 22–29.

51. Huang, G., and Eckrich, S. (2021). Quantitative fluorescent in situ hybridization reveals differential transcription profile sharpening of endocytic proteins in cochlear hair cells upon maturation. Front. Cell. Neurosci. *15*, 643517.

52. Yoshimura, H., Shibata, S.B., Ranum, P.T., and Smith, R.J.H. (2018). Enhanced viral-mediated cochlear gene delivery in adult mice by combining canal fenestration with round window membrane inoculation. Sci. Rep. *8*, 2980.

53. Li, S.L., Chen, X., Wu, T., Zhang, X.W., Li, H., Zhang, Y., and Ji, Z.Z. (2018). Knockdown of TMPRSS3 inhibits gastric cancer cell proliferation, invasion and EMT via regulation of the ERK1/2 and PI3K/Akt pathways. Biomed. Pharmacother. *107*, 841–848.

54. Wang, J.Y., Jin, X., and Li, X.F. (2018). Knockdown of TMPRSS3, a transmembrane serine protease, inhibits proliferation, migration, and invasion in human nasopharyngeal carcinoma cells. Oncol. Res. *26*, 95–101.

55. Guipponi, M., Toh, M.Y., Tan, J., Park, D., Hanson, K., Ballana, E., Kwong, D., Cannon, P.Z.F., Wu, Q., Gout, A., et al. (2008). An integrated genetic and functional analysis of the role of type II transmembrane serine proteases (TMPRSSs) in hearing loss. Hum. Mutat. *29*, 130–141.

56. Tang, P.C., Alex, A.L., Nie, J., Lee, J., Roth, A.A., Booth, K.T., Koehler, K.R., Hashino, E., and Nelson, R.F. (2019). Defective Tmprss3-associated hair cell degeneration in inner ear organoids. Stem Cell Rep. *13*, 147–162.

57. Li, Y., Peng, A., Ge, S., Wang, Q., and Liu, J. (2014). miR-204 suppresses cochlear spiral ganglion neuron survival in vitro by targeting TMPRSS3. Hear. Res. *314*, 60–64.

58. Chen, Y.S., Cabrera, E., Tucker, B.J., Shin, T.J., Moawad, J.V., Totten, D.J., Booth, K.T., and Nelson, R.F. (2022). TMPRSS3 expression is limited in spiral ganglion neurons: implication for successful cochlear implantation. J. Med. Genet. *59*, 1219–1226.

59. Eppsteiner, R.W., Shearer, A.E., Hildebrand, M.S., Deluca, A.P., Ji, H., Dunn, C.C., Black-Ziegelbein, E.A., Casavant, T.L., Braun, T.A., Scheetz, T.E., et al. (2012). Prediction of cochlear implant performance by genetic mutation: the spiral ganglion hypothesis. Hear. Res. *292*, 51–58.

60. Holder, J.T., Morrel, W., Rivas, A., Labadie, R.F., and Gifford, R.H. (2021). Cochlear implantation and electric acoustic stimulation in children with TMPRSS3 genetic mutation. Otol. Neurotol. *42*, 396–401.

61. Colella, P., Ronzitti, G., and Mingozzi, F. (2018). Emerging issues in AAV-mediated in vivo gene therapy. Mol. Ther. Methods Clin. Dev. *8*, 87–104.

62. Tao, Y., Huang, M., Shu, Y., Ruprecht, A., Wang, H., Tang, Y., Vandenberghe, L.H., Wang, Q., Gao, G., Kong, W.J., and Chen, Z.Y. (2018). Delivery of adeno-associated virus vectors in adult mammalian inner-ear cell subtypes without auditory dysfunction. Hum. Gene Ther. *29*, 492–506.

63. Suzuki, J., Hashimoto, K., Xiao, R., Vandenberghe, L.H., and Liberman, M.C. (2017). Cochlear gene therapy with ancestral AAV in adult mice: complete transduction of inner hair cells without cochlear dysfunction. Sci. Rep. *7*, 45524.

64. Omichi, R., Yoshimura, H., Shibata, S.B., Vandenberghe, L.H., and Smith, R.J.H. (2020). Hair cell transduction efficiency of single- and dual-AAV serotypes in adult murine cochleae. Mol. Ther. Methods Clin. Dev. *17*, 1167–1177.

65. Nass, S.A., Mattingly, M.A., Woodcock, D.A., Burnham, B.L., Ardinger, J.A., Osmond, S.E., Frederick, A.M., Scaria, A., Cheng, S.H., and O'Riordan, C.R. (2018). Universal method for the purification of recombinant AAV vectors of differing serotypes. Mol. Ther. Methods Clin. Dev. *9*, 33–46.

66. Noh, B., Rim, J.H., Gopalappa, R., Lin, H., Kim, K.M., Kang, M.J., Gee, H.Y., Choi, J.Y., Kim, H.H., and Jung, J. (2022). In vivo outer hair cell gene editing ameliorates progressive hearing loss in dominant-negative Kcnq4 murine model. Theranostics *12*, 2465–2482.

67. Shu, Y., Tao, Y., Wang, Z., Tang, Y., Li, H., Dai, P., Gao, G., and Chen, Z.Y. (2016). Identification of adeno-associated viral vectors that target neonatal and adult mammalian inner ear cell subtypes. Hum. Gene Ther. *27*, 687–699.

68. Sievers, F., Wilm, A., Dineen, D., Gibson, T.J., Karplus, K., Li, W., Lopez, R., McWilliam, H., Remmert, M., Söding, J., et al. (2011). Fast, scalable generation of high-quality protein multiple sequence alignments using Clustal Omega. Mol. Syst. Biol. *7*, 539.

69. Shearer, A.E., Tejani, V.D., Brown, C.J., Abbas, P.J., Hansen, M.R., Gantz, B.J., and Smith, R.J.H. (2018). In vivo electrocochleography in hybrid cochlear implant users implicates TMPRSS3 in spiral ganglion function. Sci. Rep. *8*, 14165.

70. Miyagawa, M., Nishio, S.Y., Sakurai, Y., Hattori, M., Tsukada, K., Moteki, H., Kojima, H., and Usami, S.I. (2015). The patients associated with TMPRSS3 mutations are good candidates for electric acoustic stimulation. Ann. Otol. Rhinol. Laryngol. *124* (*Suppl 1*), 193S–204S.

71. Müller, M.K., Jovanovic, S., Keine, C., Radulovic, T., Rübsamen, R., and Milenkovic, I. (2019). Functional development of principal neurons in the anteroventral cochlear nucleus extends beyond hearing onset. Front. Cell. Neurosci. *13*, 119.

72. Xue, Y., Hu, X., Wang, D., Li, D., Li, Y., Wang, F., Huang, M., Gu, X., Xu, Z., Zhou, J., et al. (2022). Gene editing in a Myo6 semi-dominant mouse model rescues auditory function. Mol. Ther. *30*, 105–118.

73. György, B., Nist-Lund, C., Pan, B., Asai, Y., Karavitaki, K.D., Kleinstiver, B.P., Garcia, S.P., Zaborowski, M.P., Solanes, P., Spataro, S., et al. (2019). Allele-specific gene editing prevents deafness in a model of dominant progressive hearing loss. Nat. Med. *25*, 1123–1130.

74. Xing, Y., Samuvel, D.J., Stevens, S.M., Dubno, J.R., Schulte, B.A., and Lang, H. (2012). Age-related changes of myelin basic protein in mouse and human auditory nerve. PLoS One *7*, e34500.

75. Ivarsdottir, E.V., Holm, H., Benonisdottir, S., Olafsdottir, T., Sveinbjornsson, G., Thorleifsson, G., Eggertsson, H.P., Halldorsson, G.H., Hjorleifsson, K.E., Melsted, P., et al. (2021). The genetic architecture of age-related hearing impairment revealed by genome-wide association analysis. Commun. Biol. *4*, 706.

76. Ołdak, M., Lechowicz, U., Pollak, A., Oziębło, D., and Skarżyński, H. (2019). Overinterpretation of high throughput sequencing data in medical genetics: first evidence against TMPRSS3/GJB2 digenic inheritance of hearing loss. J. Transl. Med. *17*, 269.

77. Leone, M.P., Palumbo, P., Ortore, R., Castellana, S., Palumbo, O., Melchionda, S., Palladino, T., Stallone, R., Mazza, T., Cocchi, R., and Carella, M. (2017). Putative TMPRSS3/GJB2 digenic inheritance of hearing loss detected by targeted resequencing. Mol. Cell. Probes *33*, 24–27.

78. Sena-Esteves, M., and Gao, G. (2020). Introducing genes into mammalian cells: viral vectors. Cold Spring Harb. Protoc. *2020*, 095513. https://doi.org/10.1101/pdb.top095513.

79. Liang, S.Q., Walkey, C.J., Martinez, A.E., Su, Q., Dickinson, M.E., Wang, D., Lagor, W.R., Heaney, J.D., Gao, G., and Xue, W. (2022). AAV5 delivery of CRISPR-Cas9 supports effective genome editing in mouse lung airway. Mol. Ther. *30*, 238–243.

80. Hu, Z., Ulfendahl, M., and Olivius, N.P. (2004). Central migration of neuronal tissue and embryonic stem cells following transplantation along the adult auditory nerve. Brain Res. *1026*, 68–73.

81. Zhang, L., Jiang, H., and Hu, Z. (2011). Concentration-dependent effect of nerve growth factor on cell fate determination of neural progenitors. Stem Cells Dev. *20*, 1723–1731.